CrossMark

Thermolysis Synthesis of Pure Phase Nano-Sized Cobalt(II) Oxide from Novel Cobalt(II)-Pyrazole Discrete Nano Coordination Compound

Younes Hanifehpour[1] · Behzad Soltani[2] · Babak Mirtamizdoust[3] · Bamin Khomami[4] ·
Sang Woo Joo[1]

Abstract Nano-structures of a new discrete coordination compound of divalent cobalt with the pyrazol (pzH) containing the terminal isothiocyanate anions, $[Co(pzH)_2(NCS)_2]$ (**1**), with discrete molecular architecture in solid state was synthesized by a sonochemical method. The new nanostructure was characterized by scanning electron microscopy, transmission electron microscopy, X-ray photoelectron spectroscopy, X-ray powder diffraction, IR, and elemental analysis. The supramolecular features in these complexes are guided and controlled by weak directional intermolecular interactions. The discrete molecules interact with each other through labile interactions creating a 3D supramolecular framework. The CoO nanoparticles were obtained by thermolysis of **1** at 180 °C with oleic acid as a surfactant.

1 Introduction

Design and synthesis of discrete coordination compound have attracted extensive interest for their great application potential for separation, recognition, catalysis, and sensor technologies [1].

In the past decade, the rational design and syntheses of novel coordination supramolecular compounds have made considerable progress in the field of crystal engineering and supramolecular chemistry [2, 3].

Coordination bonding, electrostatic interactions and versatile hydrogen bonding, π–π stacking have been commonly recognized in constructing extended networks [4]. The creation of new molecules is a main goal of chemistry, and of great contribution to human well-being and prosperity. Molecules are architectures of atoms, while crystal engineering of crystalline solids deals with targeted structures built from molecules. Discrete molecular architecture (DMA) involves the synthesis of discrete, supramolecular entities that exist both in solid state and the solution [5, 6]. One of the more prevalent and effective design strategies is directional-bonding approach. In this building block-based methodology, complementary subunits are reacted in the appropriate ratio to give a final aggregate whose size and structure are dictated by the molecular information stored within the precursors themselves [7, 8]. Heterocyclic nitrogen ligands such as pyrazole-based compounds are known for their interesting coordination chemistry as co-ligands, often giving di- or polynuclear complexes [9]. Some examples of such compounds are [Cu(μ-Cl)(2-

✉ Younes Hanifehpour
  younes.hanifehpour@gmail.com; y_hanifehpour@yu.ac.kr

✉ Babak Mirtamizdoust
  Babakm.tamizdoust@gmail.com

✉ Sang Woo Joo
  swjoo1@gmail.com

[1] School of Mechanical Engineering, Yeungnam University, Gyeongsan 712-749, South Korea

[2] Department of Chemistry, Faculty of Basic Sciences, Azarbaijan Shahid Madani University, Tabriz, Iran

[3] Department of Chemistry, Faculty of Science, University of Qom, PO Box 37185-359, Qom, Iran

[4] Department of Chemical and Biomolecular Engineering, University of Tennessee, Knoxville, TN 37996, USA

Apy)(PPh3)]$_2$ (2-Apy = 2-aminopyridine) [9], [CuI(PPh3)(Py)]$_2$ [10] and [Cu$_2$(5-aminomethyl-3-methylpyrazole) Cl$_4$] [11], The halides in these complexes act as bridging ligands, as also observed in other complexes such as [Cu$_2$L$_2$Cl$_4$] and [Cu$_2$L$_2$Br$_2$] (L = 3,5-dimethyl-1-thiocarbox-amide pyrazole) [12]. We have synthesized and characterized a number of copper complexes containing pyrazole-based ligands [13]. Also, other researchers have reported several metal coordination compound based on pyrazole [14–19].

The nano-particles of CoO have been used for several applications like anode materials for advanced Li-ion battery [20], pigments [21], and are expected to play a major role in further improving the optical and electrical properties [22].

Recently we have reported some metal–azido complexes and synthesized nano metal coordination compounds [23–25]. As a continuation of the previous study, in this paper we extend these experimental and theoretical studies to investigate the interactions of isothiocyanate anion with cobalt(II) ions in the presence of pyrazole ligand and describe a simple synthetic sonochemical preparation of nano-structures of this coordination compound and its use in the preparation of CoO nanoparticles.

2 Experimental

2.1 Materials and Physical Measurements

Co(CH$_3$COO)$_2$·4H$_2$O, KSCN and pyrazole (pzH), were obtained from Sigma-Aldrich. An Elementar Vario Microanalyzer CHN–O-rapid analyzer was used for C, H and N elemental analyses of the samples. The IR spectra were performed on a Bruker Vector 22 FT-IR spectrometer by using KBr disks in the 4000–400 cm^{-1} range. X-ray powder diffraction (XRD) measurements were performed using an X'pert diffractometer manufactured by the Panalytical, with monochromatized Cu-k$_\alpha$ radiation. Simulated XRD powder patterns based on single crystal data were prepared using Mercury [26]. The crystallite sizes of selected samples were estimated using the Scherrer formula. The morphology of samples after gold coating was investigated using a scanning electron microscope (Philips XL 30). A multiwave ultrasonic generator (Sonicator_3000; Misonix Inc., Farmingdale, NY, USA), equipped with a converter/transducer and titanium oscillator (horn), 12.5 mm in diameter, operating at 20 kHz with a maximum power output of 600 W at room temperature for 1 h, was used for the ultrasonic irradiation. Thermal stability studies were performed on TGA/SDTA-851e thermogravimetric analyzer (Mettler-Toledo Company, Switzerland). The chemical composition and evaluation of the chemical state of the final product was performed by X-ray photoelectron spectroscopy (XPS) (K-ALPHA, UK).

2.2 Preparation of [Co(pzH)$_4$(NCS)$_2$] (1)

To prepare the nano-structure of [Co(pzH)$_2$(NCS)$_2$] (1), a 15 mL of a 0.1 M solution of Co(CH$_3$COO)$_2$·4H$_2$O in H$_2$O was positioned in a high-density ultrasonic probe, operating at 20 kHz with a maximum power output of 600 W. Into these solution 30 mL of a 0.1 M solution of the ligands pyrazole and 45 mL of a 0.1 M solution of KSCN were added dropwise. The obtained precipitates were filtered off, washed with water and then dried in air.

Product 1: d.p. = 294 °C. Analysis: found C: 38.00, H: 4.00, N: 31.00 %, Calculated for C$_{14}$H$_{16}$CoN$_{10}$S$_2$: C: 37.58, H: 3.60, N: 31.31 %.

IR (selected bands; in cm^{-1}): 1530 *m* and 1638 *w* [ν (C=N and C=C)]. 2100*vs* (ν$_{asym}$ of –NCS), 2145*vs* (ν$_{asym}$ of –NCS), 3125 s [ν (C–H)], 3212 and 3355 *s* (ν (N–H)) [27].

To isolate single crystals of [Co(pzH)$_2$(NCS)$_2$] (1), pyrazole (0.14 g, 2 mmol) was placed in one arm of a branched tube [28] and Co(CH$_3$COO)$_2$·4H$_2$O (0.25 g, 1 mmol) and potassium thiocyanate (0.19 g, 2 mmol) in the other. Methanol was then carefully added to fill both arms, the tube sealed and the ligand-containing arm immersed in a bath at 60 °C, while the other was left at ambient temperature. After 3 weeks, crystals (d.p. 295 °C) suitable for an X-ray structure determination had deposited in the arm at ambient temperature. They were then filtered off, washed with acetone and ether, and air dried. Yield: 81 %). Analysis: found C: 38.00, H: 4.00, N: 31.10 %, Calculated for C$_{14}$H$_{16}$CoN$_{10}$S$_2$: C: 37.58, H: 3.60, N: 31.31 %.
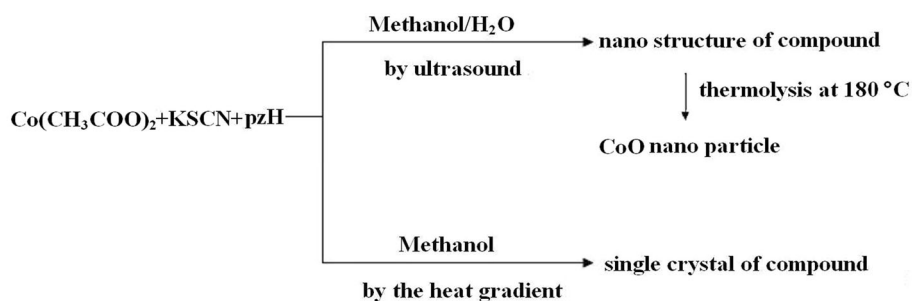
IR (selected bands; in cm^{-1}): 1530 *m* and 1635 *w* [ν (C=N and C=C)]. 2100*vs* (ν$_{asym}$ of –NCS), 2145*vs* (ν$_{asym}$ of –NCS), 3125 s [ν (C–H)], 3215 and 3357 *s* (ν (N–H)) [27].

2.3 Synthesis of CoO Nanoparticles

The 0.1 mmol of the [Co(pzH)$_2$(NCS)$_2$] (1) 1 were dispersed in 1.50 mL oleic acid to form a homogenous emulsion solution. This solution was stirring for 30 min at mild heating (60 °C) and then heated to 180 °C in an electric furnace under air atmosphere for 2 h. Two mL of toluene and a large excess of EtOH (20 ml) were added to the reaction solution. Nanoparticles of CoO was separated after washing with ethanol. The solid was washed with EtOH and dried under air atmosphere (Yield: 54 %).

2.4 Crystallography

A crystal of the compound (light yellow, plate-shaped, size 0.20 × 0.10 × 0.10 mm) was mounted on a glass fiber with grease and cooled to −93 °C in a stream of nitrogen gas controlled with Cryostream Controller 700. Data collection was performed on a Bruker SMART APEX II X-ray diffractometer with graphite-monochromated Mo-K$_\alpha$

Scheme 1 Materials produced and synthetic methods

Co(CH₃COO)₂+KSCN+pzH —

Methanol/H₂O by ultrasound → nano structure of compound

thermolysis at 180 °C ↓

CoO nano particle

Methanol by the heat gradient → single crystal of compound

radiation (λ = 0.71073 Å), operating at 50 kV and 30 mA over 2θ ranges of 3.92–52.00°. No significant decay was observed during the data collection. Data were processed on a PC using the Bruker AXS Crystal Structure Analysis Package [29–33]: Data collection: APEX2 [33]; cell refinement: SAINT [32]; data reduction: SAINT [32]; absorption correction: SADABS [30]; structure solution: XPREP [31] and SHELXTL [29]; structure refinement: SHELXTL; molecular graphics: SHELXTL; publication materials: SHELXTL. Neutral atom scattering factors were taken from Cromer and Waber [34]. The crystal is monoclinic with space group, C2/c based on the systematic absences, E statistics and successful refinement of the structure. The structure was solved by direct methods. Full-matrix least-square refinements minimizing the function $\sum w\left(F_o^2 - F_c^2\right)^2$ were applied to the compound. All non-hydrogen atoms were refined anisotropically. All H atoms were placed in geometrically calculated positions, with C–H = 0.95 (aromatic), and 0.98(CH₃) Å, and refined as riding atoms, with Uiso(H) = 1.5UeqC(CH₃) or 1.2 UeqC (other C).

2.5 Computational Details

The geometry of the complex **1** has been optimized using the B3LYP density functional model and X-ray structure data. In these calculations the 3-21G* basis set was used for C and H atoms, while the 6-31G* basis set was used for S and N, atoms. For the Co atoms, the LanL2DZ valence and effective core potential functions were used [35, 36].[1] All DFT calculations were performed with the Gaussian 98 R-A.9 package [37].

3 Results and Discussion

The reaction between "pzH" and cobalt(II) acetate and potassium thiocyanate using two different routes provided crystalline materials of the general formula [Co(pzH)₂(NCS)₂]

---

[1] A description of the basis sets and theory level used in this work can be found in the following Reference [36].

Table 1 Experimental FT-IR frequencies (cm⁻¹) for [Co(pzH)₂ (NCS)₂], compared with the theoretical frequencies obtained from DFT calculations

Assignment	Experimental	Calculated
ν (C=N and C=C)	1530 *m* and 1635 *w*	1545 and 1640
ν (N–H)	3215 and 3357 s	32000 and 3350
ν$_{asym}$ of –NCS	2100*vs* and 2145*vs*	2110 and 2180
ν (C–H)	3125 s	3120
ν (Co–N)		398
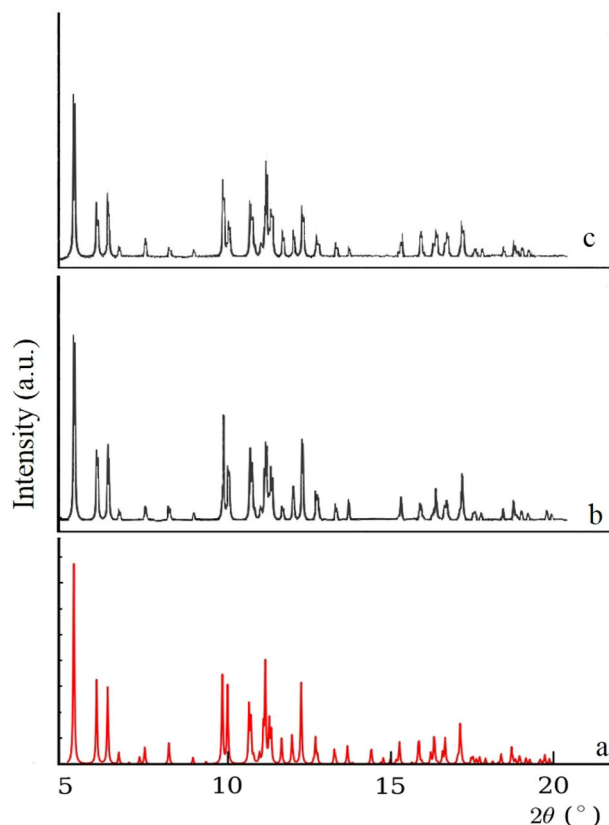
Fig. 1 The XRD patterns of **a** Computed from single crystal X-ray data of compound **1**; **b** single crystal of compound 1; and **c** nano-structure of compound 1

(**1**). Scheme 1 gives an overview of the methods used for the synthesis of [Co(pzH)₂(NCS)₂] (**1**) using two different routes.

Nano structure of compound **1** were obtained by ultrasonic irradiation in a water/methanolic solution and single crystalline material was obtained using a heat gradient applied to a solution of the reagents (the ''branched tube method'') [28]. The elemental analysis and IR spectra of the nano structure and of the single crystalline material are indistinguishable. The selected spectral data and the corresponding data obtained from DFT calculations are given in Table 1. The IR spectra of the nano-structures and the single crystalline materials show the characteristic absorption bands of the "pzH" ligands and isothiocyanate anions. The strong doublet absorption band centered at ca. 2125–2145 cm⁻¹ is assigned to the ν_{asy} (NCS̄). The relatively band around 3215 and 3357 cm⁻¹ is attributed to the absorption of the N–H group of "pzH" ligands. The absorption band in the frequency range 1530–1635 cm⁻¹ correspond to rings vibrations of "pzH" ligand [27].
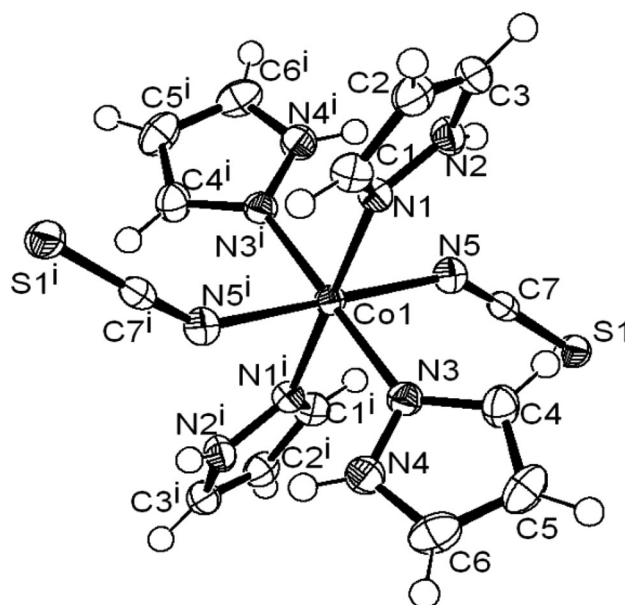
Figure 1 shows the simulated XRD pattern from the single crystal X-ray data of compound **1** (Fig. 1a), in comparison with the XRD pattern of single crystal of

Table 2 Crystal data and structure refinement for [Co(pzH)₂(NCS)₂] (**1**)

Chemical formula	C₁₄H₁₆CoN₁₀S₂
M_r	447.42
Crystal system, space group	Monoclinic, C2/c
Temperature (K)	100
a, b, c (Å)	11.382 (3), 12.270 (3), 14.206 (3)
β (°)	105.582 (2)
V (Å³)	1911.2 (8)
Z	4
Radiation type	Mo Kα
μ (mm⁻¹)	1.14
Crystal size (mm)	0.20 × 0.10 × 0.10
T_{min}, T_{max}	0.804, 0.895
No. of measured, independent and observed [I > 2σ(I)] reflections	7491, 2076, 1951
R_{int}	0.028
(sin θ/λ)ₘₐₓ (Å⁻¹)	0.642
R[F² > 2σ(F²)], wR(F²), S	0.025, 0.071, 0.90
No. of reflections	2076
No. of parameters	124
H-atom treatment	H-atom parameters constrained
Δ⟩ₘₐₓ, Δ⟩ₘᵢₙ (e Å⁻³)	0.32, −0.30

Fig. 2 SEM photograph of [Co(pzH)₂(NCS)₂] (**1**) nano flowers at different magnifications

Fig. 3 Fragment of the discrete coordination compound (DCC) of **1**

Table 3 Selected bond lengths [Å] and angles [°] for [Co(pzH)$_2$(NCS)$_2$] (**1**) (Experimental data belong to the solid phase, whereas the calculated data correspond to the isolated molecule in gas-phase)

	Experimental	Calculated		Experimental	Calculated
Co1–N3^i	2.1134 (13)	2.120	Co1–N1^i	2.1356 (13)	2.140
Co1–N3	2.1134 (13)	2.120	Co1–N5^i	2.1472 (14)	2.151
Co1–N1	2.1356 (13)	2.140	Co1–N5	2.1472 (14)	2.151
N3–Co1–N3^i	180.0	180	N1–Co1–N5^i	91.07 (5)	90
N1–Co1–N3^i	92.01 (5)	94	N1^i–Co–N5^i	88.93 (5)	86
N1^i–Co1–N3^i	87.99 (5)	89	N3–Co1–N5^i	89.36 (5)	90
N1–Co1–N3	87.99 (5)	89	N3^i–Co1–N5	89.36 (5)	90
N3–Co1–N1^i	92.01 (5)	94	N1–Co1–N5	88.93 (5)	86
N1–Co1–N1^i	180.0	180	N1^i–Co1–N5	91.07 (5)	90
N3^i–Co1–N5^i	90.64 (5)	91.50	N5–Co1–N5^i	180.0	180
N3–Co1–N5	90.64 (5)	91.50			

Symmetry code(s): (i) −x + 1/2, −y + 1/2, −z + 1

[Co(pzH)$_2$(NCS)$_2$] (Fig. 1b) and a typical sample of compound **1** prepared by the sonochemical process (Fig. 1c). Acceptable matches, with slight differences in 2θ, were observed for the simulated and experimental powder X-ray diffraction patterns. This indicates that the compound obtained via crystalline phase is identical to that obtained by sonochemical approach.

The morphology of compound 1 prepared by the sonochemical method is very interesting. It is composed of flower sheets with thickness of about 10–40 nm (Fig. 2).

X-ray structure of complex **1** (Table 2), revealed the composition and stereochemistry of a fundamental building block, having a formula of [Co(pzH)$_2$(NCS)$_2$].

The determination of the structure of [Co(pzH)$_2$(NCS)$_2$], (**1**) showed that the complex crystallizes in the monoclinic system with space group *C2/c*, taking the form of a discrete coordination compound (DCC) in the solid state (Fig. 3). Table 3 shows the experimental value of the selected bonds lengths and angles of the complex.

The cobalt(II) atom is coordinated by four nitrogen atoms of four "pzH" ligands with the Co–N distance of 2.1134 (13), 2.1356 (13), 2.1134 (13) and 2.1356 (13) Å and two nitrogen atoms of two isothiocyanate terminal anions with the similar Co–N distances of 2.1472 (14) Å, with a CoN$_6$ donor set. Thus, the coordination number of the cobalt(II) atom is six, with symmetrical coordination sphere (Fig. 4).

There are several supramolecular interactions observed in structure. There are N–H···S interactions, π···H–C interactions amongst the weak non-covalent contacts belonging to fragments of adjacent, distances values of these interactions (see Table 4) that suggest relatively strong interactions within this class of weak non-covalent contacts [38]. With expanding all the week supramolecular interactions, the discrete coordination compound interacts
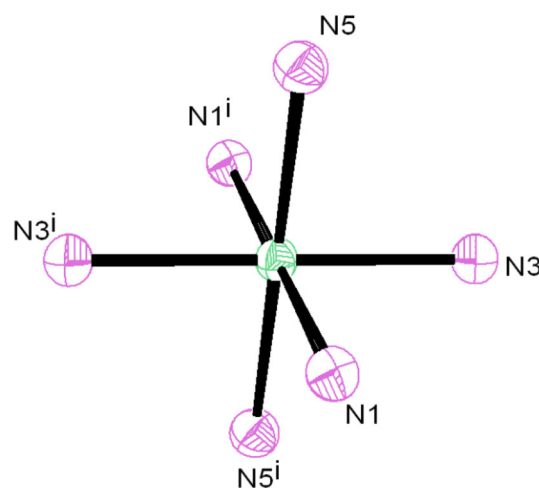

Fig. 4 Schematic representation of Co^{II} environment

Table 4 Selected non-covalent contacts in the crystal structure of **1**

N–H···S	H···N Å	N···S Å	<S···H–N°
N2–H1··· S1	2.601	3.344	45.35
N2^i–H1^i··· S1^i	2.601	3.344	45.35
C–H···π	π ···H Å	C··· π Å	< π ···H–C°
C5–H5··· π	2.867	3.125	85.00
C5^i–H5^i··· π	2.867	3.125	85.00
C4–H4··· π	2.706	3.020	94.18

with neighbors and the structure extended to 3D supramolecular networks (Fig. 5).

The mechanism of formation of nano structures needs to be further investigated, however it may be a result of the crystal structure of the compound which is, *i.e.* the packing of the structure on a molecular level might have influence on the morphology of the nano-structure of the compound [39–42].
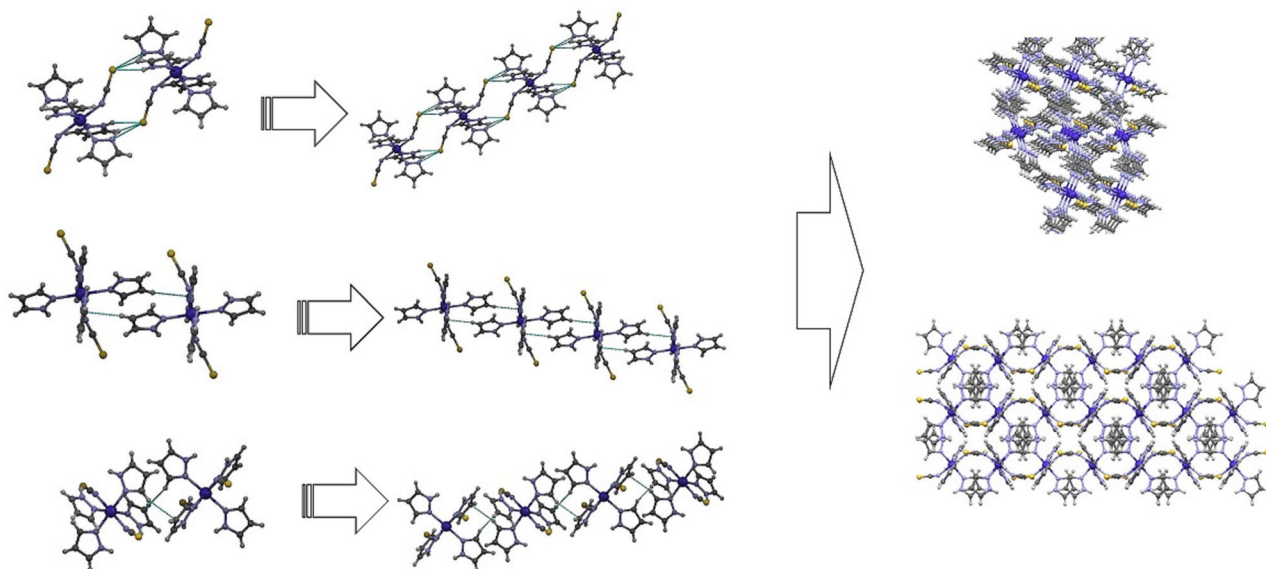
Fig. 5 From discrete coordination compound to supramolecular coordination networks via labile interactions

3.1 DFT Calculations

The calculated structural parameters are listed in Table 3. It should be noted that the experimental data belong to the solid phase, whereas the calculated data correspond to the isolated molecule in gas-phase. However, the experimental and computational data in Table 3 clearly show that both data only slightly differ from each other. For example, the largest difference between experimental and calculated Co1–N3 length is about 0.007 Å, while the largest deviation of ca. 2.3$\mathring{1}$occurs for the N1^i–Co1–N5^i angle. As a result, the calculated geometrical parameters represent a good approximation.

The computed IR frequencies are listed in Table 1 together with the experimentally determined frequencies. The assignment of the ν(Co–N) vibration is based on the theoretically calculated frequency with the frequency value 398 cm^{-1} for a cobalt complex [Co(pzH)$_2$(NCS)$_2$].

The NBO charges of cobalt(II) and of the coordinated atoms were also calculated. The positive charge of the cobalt(II) ions was 0.927. The charges of the coordinated nitrogen atom of the "pzH" ligands were −0.313 and −0.314, respectively, whereas the nitrogen atoms of both thiocyanate anions have similar charges: (N5^i and N5 = −0.602).

The calculations indicate that complex **1** has 115 occupied molecular orbitals (MOs) per [Co(pzH)$_2$ (NCS)$_2$] unit. The value of the energy separation between the highest occupied molecular orbital (HOMO) and the lowest unoccupied molecular orbital (LUMO) was calculated. Figure 6 shows the HOMO and LUMO for the cobalt(II) complex. As seen in Fig. 6, the HOMO of the title complex is principally localized on the cobalt and isothiocynate atoms, whereas
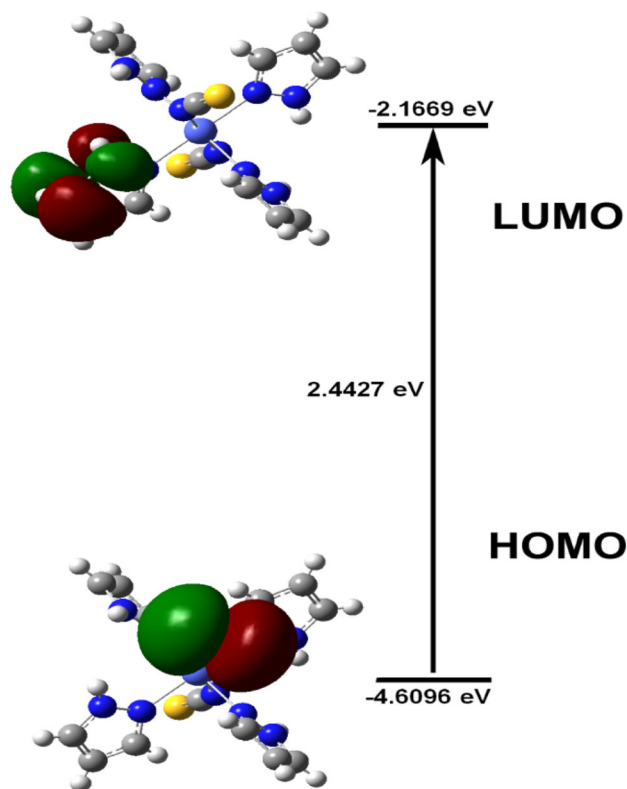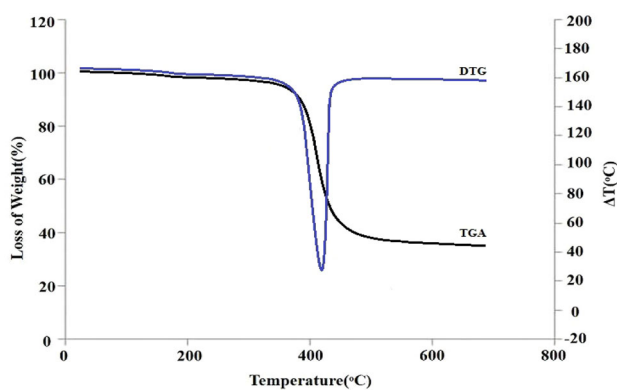

Fig. 6 Frontier molecular orbitals for a unit of [Co(pzH)$_2$(NCS)$_2$] (**1**)

the LUMO is approximately delocalized on all atoms of one "pzH" ligand. The calculated HOMO–LUMO gap is 2.4427 eV.

UV–Vis diffuse reflectance spectrum is used to probe the optical absorption property, as shown in Fig. 7a. The
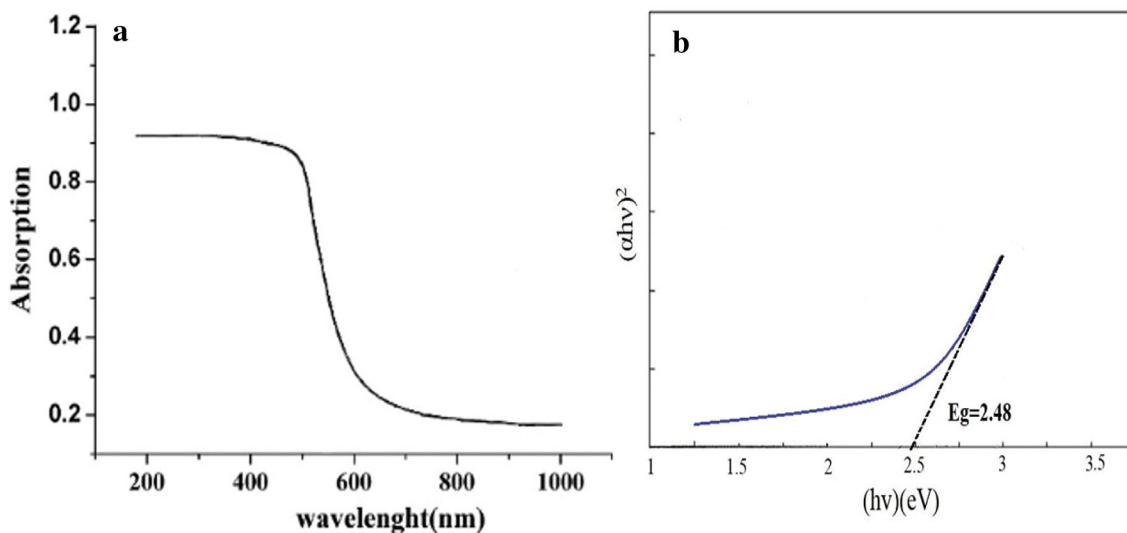
Fig. 7 **a** DRS spectra and **b** Tauc's plot of the optical absorption spectrum of complex 1

Fig. 8 Thermal behavior of compound **1**

band-gap energies of complex **1** was calculate by Tauc's equation [43]:

$$\alpha h\upsilon = A \left(h\upsilon - E_g\right)^n,$$

where α is the absorption coefficient, $h\upsilon$ is the photon energy, E_g is the direct band gap energy, and A is a constant. The indirect optical energy gap can be obtained from the intercept of the resulting linear region with the energy axis. The calculated band gap for the complex 1 is about $E_g = 2.48$ eV and close to value calculated by DFT ($E_g = 2.44$ eV).

To examine the thermal stability of compound **1**, thermogravimetric (TG) analysis and differential thermal
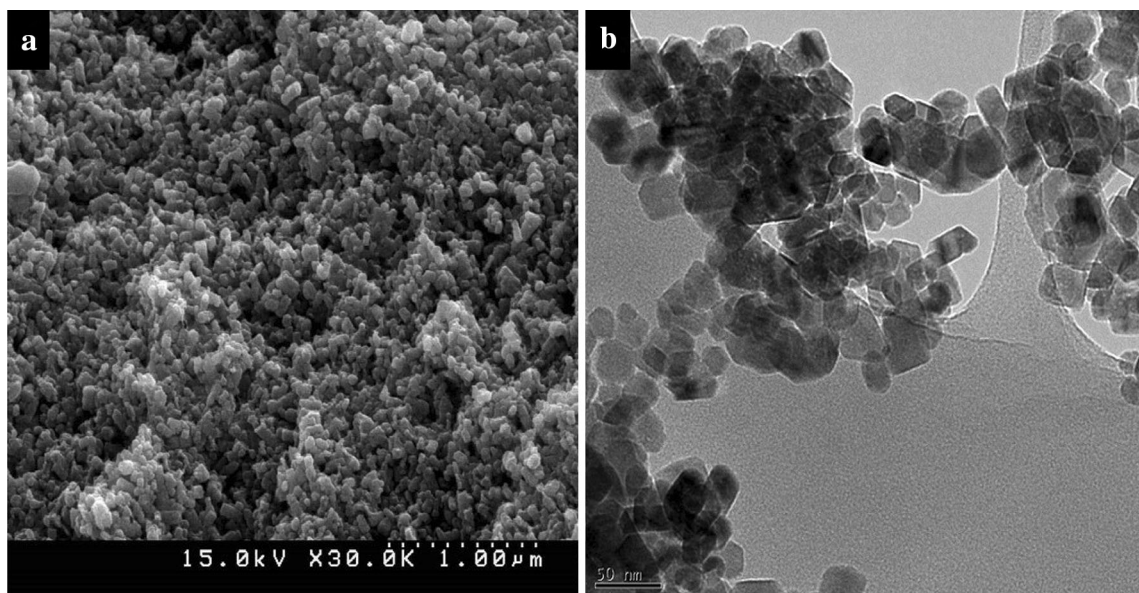
Fig. 9 SEM (**a**) and TEM (**b**) photographs of CoO nanoparticles (produced by thermolysis of nanostructure)
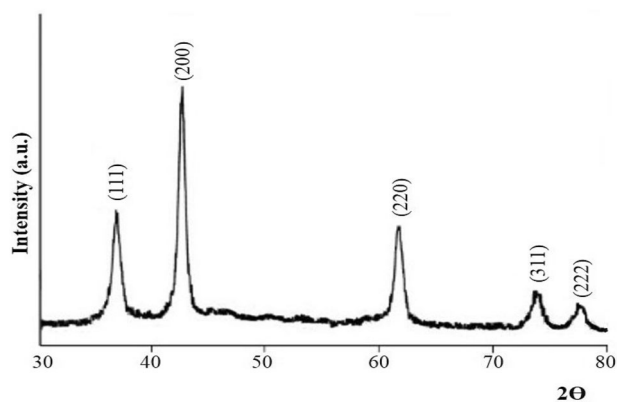
Fig. 10 XRD patterns of CoO after thermolysis of **1**

analysis (DTA) were carried out between 10 and 780 °C in an argon flow (Fig. 8). The compound **1** was stable up to 345 °C, at which temperature the decomposition process started. The DTA curve indicates that decomposition and thermolysis of **1** occurs with exothermic effects at 345 °C. The final product upon thermal decomposition of compound **1**, based on the XPS spectrum and XRD pattern, is CoO.
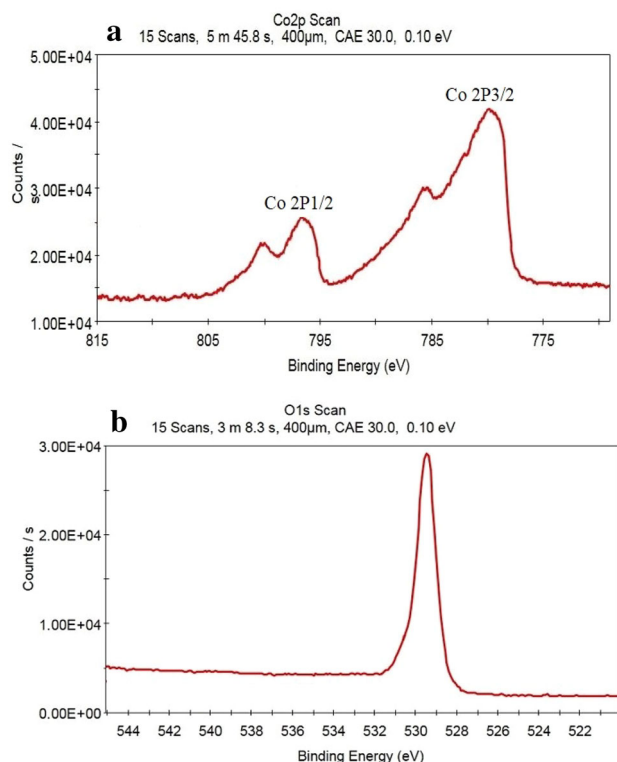
3.2 Nano Structure of CoO

Nano-powders of CoO were obtained from the decomposition of the precursor **1** in oleic acid as surfactant at 180 °C, under air atmosphere. The morphology and size of the as-prepared CoO samples were further investigated using Scanning Electron Microscope (SEM) and Transmission Electron Microscope (TEM). This process produces regular shape of cobalt(II) oxide nano-particles with the diameter about 15–50 nm (Fig. 9). The final products by decomposing of the compound **1** is, based on their XRD patterns (Fig. 10), match with the standard pattern of cubic structure of CoO (a = 4.26 Å) (JCPDS 9-0402).

Figure 11 shows the XPS spectra of CoO nanoparticles. The two asymmetric peaks centered at 780.8 and 796.2 eV are due to the transitions of 2P3/2 and 2P1/2, respectively, and are attributed to Co^{2+} ions in CoO [44, 45]. The corresponding O 1 s peak of the Co oxide is observed at 530 eV [44, 45].

4 Conclusions

In this work, a novel Co(II) discrete coordination compound containing a neutral pyrazole ligand and isothiocyanate anion is described together with a simple sonochemical preparation of this nano coordination compound.The crystal structure of the complex indicates the form of a discrete molecular architecture (DMA) in the solid state. With several supramolecular interactions, the (DCCs) interacts with neighbors and the structure extended to 3D supramolecular coordination networks.

A theoretical study of the title coordination compound was undertaken to examine its electronic structure, which allowed computations of bond distances and angles and vibrational frequencies in good agreement with the experimental data. The nano-structures of this coordination compound used as precursor in the preparation of CoO nanoparticles.

5 Supplementary Material

Crystallographic data for the structures reported in this paper has been deposited with the Cambridge Crystallographic Data Centre as supplementary publication CCDC-1062455 for [Co(pzH)$_2$(NCS)$_2$] (**1**). Copies of the data can be obtained on application to CCDC, 12 Union Road, Cambridge CB2 1EZ, UK [Fax: +44-1223-336033; E-Mail: de-posit@ccdc.cam.ac.uk].

Fig. 11 XPS spectrum of CoO nanoparticles

References

1. N. Li, F. Jiang, L. Chen, X. Li, Q. Chen, M. Hong, Chem. Commun. **47**, 2327 (2011)
2. B. Moulton, M.J. Zaworotko, Chem. Rev. **101**, 1629 (2001)
3. C.J. Janiak, Dalton Trans. **2003**, 2781 (2003)
4. A.V. Khripun, S.I. Selivanove, V.Y. Kukushkin, M. Haukka, Inorg. Chim. Acta **359**, 320 (2006)
5. S.K. Seth, Inorg. Chim. Acta **43**, 60 (2014)
6. J.-M. Lehn, *Supramolecular Chemistry, Concepts and Perspectives* (VCH, Weinheim, 1995), pp. 139–160
7. M. Schweiger, S.R. Seidel, A.M. Arif, P.J. Stang, Angew. Chem. Int. Ed. **40**, 3467 (2001)
8. K. Ohno, A. Nagasawa, T. Fujihara, Dalton Trans. **44**, 368 (2015)
9. Q.H. Jin, L.L. Song, R. Wong, C.L. Zhang, X. Zuo, X.M. Lu, Polyhedron **29**, 441 (2010)
10. B.K. Teo, J.C. Calabrese, Inorg. Chem. **15**, 2474 (1976)
11. A.M. Schuitema, A.F. Stassen, W.L. Driessen, J. Reedijk, Inorg. Chim. Acta **337**, 48 (2002)
12. I.R. Evans, J.A. Howard, L.E. Howard, J.S. Evans, Z.K. Jacimovic, V.M. Leovac, Inorg. Chim. Acta **357**, 4528 (2004)
13. B. Soltani, M. Hossaini Sadr, J.T. Engle, C.J. Ziegler, S.W. Joo, Y. Hanifehpour, Trans. Met. Chem. **37**, 687 (2012)
14. D.-Q. Qi, C.-M. Yu, J.-Z. You, G.-H. Yang, X.-J. Wang, Y.-P. Zhang, J. Mol. Struct. **1100**, 421 (2015)
15. N. Koch, W. Seichter, M. Mazik, Tetrahedron **71**, 8965 (2015)
16. A.M. Lopez, M. Guerrero, T. Calvet, M. Font-Bardia, J. Pons, Inorg. Chem. Commun. **55**, 51 (2015)
17. M.H. Sadhu, A. Solanki, S.B. Kumar, Polyhedron **100**, 206 (2015)
18. A. Solanki, M.H. Sadhu, S.B. Kumar, J. Mol. Struct. **1101**, 155 (2015)
19. C. Pettinari, A. Tabacaru, S. Galli, Coord. Chem. Rev. **307**, 1 (2016)
20. C.H. Chen, B.J. Hwanga, J.S. Do, J.H. Weng, M. Venkateswarlu, M.Y. Chenga, R. Santhanam, K. Ragavendran, J.F. Lee, J.M. Chen, D.G. Liu, Electrochem. Commun. **12**, 496 (2010)
21. N.M. Ahmed, D.E. El-Nashar, S.L. Abd El-Messieh, Mater. Des. **32**, 170 (2011)
22. P. Torelli, E.A. Soares, G. Renaud, S. Valeri, X.X. Guo, P. Luches, Surf. Sci. **601**, 2651 (2007)
23. Y. Hanifehpour, B. Mirtamizdoust, S.W. Joo, J. Inorg. Organomet. Polym. **22**, 916 (2012)
24. B. Mirtamizdoust, S. Ali-Asgari, S.W. Joo, E. Maskani, Y. Hanifehpour, T.H. Oh, J. Inorg. Organomet. Polym. **23**, 751 (2013)
25. Y. Hanifehpour, B. Mirtamizdoust, A. Morsali, S.W. Joo, Ultrason. Sonochem. **23**, 275 (2015)
26. Mercury 1.4.1, Copyright Cambridge Crystallographic Data Centre, Cambridge, 2001–2005
27. K. Nakamoto, *Infrared and Raman Spectra of Inorganic and Coordination Compounds*, 5th edn. (Wiley, New York, 1997), pp. 124–126
28. J.M. Harrowfield, H. Miyamae, B.W. Skelton, A.A. Soudi, A.H. White, Aust. J. Chem. **49**, 1165 (1996). **and references therein**
29. Bruker AXS Crystal Structure Analysis Package: Bruker, SHELXTL. Version 6.14. Bruker AXS Inc., Madison, Wisconsin, 2000
30. Bruker AXS Crystal Structure Analysis Package: Bruker, SADABS. Version 2008/1. Bruker AXS Inc., Madison, Wisconsin, 2008
31. Bruker AXS Crystal Structure Analysis Package: Bruker, XPREP. Version 2008/2. Bruker AXS Inc., Madison, Wisconsin, 2008
32. Bruker AXS Crystal Structure Analysis Package: . Bruker, SAINT. Version 7.68A. Bruker AXS Inc., Madison,Wisconsin, 2009
33. Bruker AXS Crystal Structure Analysis Package: Bruker, APEX2. Version 2010.3-0. Bruker AXS Inc., Madison, Wisconsin, 2010
34. D.T. Cromer, J.T. Waber, *International Tables for X-ray Crystallography* (Kynoch Press: Birmingham, 1974) Vol. 4, Table 2.2 A
35. P.J. Hay, W.R.J. Wadt, Chem. Phys. **82**, 270 (1985)
36. Foresman, J. B.; Frisch, A. E. Exploring Chemistry with Electronic Structure Methods, 2nd ed.; Gaussian Inc.: Pittsburgh, PA, 1996
37. M.J. Frisch, et al, *GAUSSIAN 98, Revision A.9* (Gaussian Inc., Pittsburgh, 1998)
38. E. Jia, L. Su, P. Liu, M. Jiang, G. Ye, J. Xu, J. Polym. Res. **21**, 548 (2014)
39. L. Aboutorabi, A. Morsali, Ultrason. Sonochem. **18**, 407 (2011)
40. M.Y. Masoomi, A. Morsali, Coord. Chem. Rev. **256**, 2921 (2012)
41. B. Mirtamizdoust, B. Shaabani, S.W. Joo, D. Viterbo, G. Croce, Y. Hanifehpour, J. Inorg. Organomet. Polym. **22**, 1397 (2012)
42. K. Akhbari, A. Morsali, Cryst. Eng. Comm. **13**, 2047 (2011)
43. R. Bhatt, I. Bhaumik, S. Ganesamoorthy, A.K. Karnal, M.K. Swami, H.S. Patel, P.K. Gupta, Phys. Status Solidi A **209**, 176 (2012)
44. J.S. Gwag, Y. Sohn, Bull. Korean Chem. Soc. **33**, 505 (2012)
45. L. Liao, Q. Zhang, Z. Su, Z. Zhao, Y. Wang, Y. Li, X. Lu, D. Wei et al., Nat. Nanotechnol. **9**, 69 (2014)